Turbulence model closures for free electroconvection

A. Kourmatzis[a,*], J.S. Shrimpton[b]

[a] *School of Aerospace, Mechanical, and Mechatronic Engineering, The University of Sydney, NSW 2006, Australia*
[b] *Engineering and the Environment, The University of Southampton, SO171BJ, UK*

Abstract

Electroconvection has been simulated in a number of recent studies, given its application in heat transfer enhancement, electrostatic atomizers and flow control. In practical applications, such as in charge injection atomizers, the electric Reynolds number can be sufficiently high such that the well-described ordered large scale electrohydrodynamic (EHD) instabilities that normally appear in electroconvection can dissipate and form into a wider distribution of length-scales. This purely electrohydrodynamically driven chaotic flow has features that resemble turbulent natural convection, and can dominate the operational regime of practical devices. Despite its practical relevance, Reynolds averaged turbulence model closures for EHD are unavailable, which currently makes direct numerical simulation the main viable option for EHD flows. Closure of EHD turbulence in free electro-convection is examined here through implementation of Reynolds stress model (RSM) closures using EHD specific timescales for the unclosed terms appearing in the turbulent scalar flux and space-charge scalar variance equations. A new closure for the highly non-linear triple correlation ($\overline{q'E'u'}$), a term which is specific to EHD, is also presented. The work demonstrates that Reynolds stress closures are a feasible modeling route for EHD flows, with errors approaching similar values as in thermal Rayleigh-Benard convection at analogous levels of turbulence.

Keywords: Electrohydrodynamics, Turbulence Closures, Free Convection

*Corresponding author

List of Symbols		Units
C	Charge Injection Strength Term	Dimensionless
C_x	Model Constants	Dimensionless
E	Electric field	V/m
k	Turbulent kinetic energy	m^2/s^2
l	reference length-scale	m
L	Length between parallel plates	m
M	EHD 'M parameter'	Dimensionless
p	pressure	Pa
Pr_E	Electric Prandtl number	Dimensionless
Q	Space charge (lower case if fluctuating component)	C/kg
Re_E	Electric Reynolds Number	Dimensionless
Sc_Q	Electric Schmidt Number	Dimensionless
T	Electric Rayleigh Number	Dimensionless
t	time	s
U	Velocity (lower case if fluctuating component)	m/s
v	Vertical velocity component	m/s
V	Voltage	V
x	local position	m
y	local vertical position	m
Greek		
ϵ	Electric permittivity	F/m
ϵ_e	Electric dissipation	m^2/s^3
ϵ_k	Dissipation of turbulent kinetic energy	m^2/s^3
η	Kolmogorov length-scale	m
κ	Ionic mobility	m^2/Vs
μ	Dynamic viscosity	Pa.s
ρ	Density	kg/m^3
τ	Time scale	s
Subscripts		
i,j,k	Tensor notation	-
o	Reference scale	-
1,2,3	Vector direction (x, y, z)	-

1. Introduction

Turbulent electrohydrodynamics has a number of practical applications, a key one being in electrostatic atomizers (Shrimpton and Yule (2001, 1999, 2004)) where it was recently experimentally demonstrated that a direct coupling exists between the inter-electrode and primary atomization zones (Kourmatzis and Shrimpton (2014); Kourmatzis et al. (2012)). Electrohydrodynamics can also have potential applications in combustion devices (Kyritsis et al. (2004); Kourmatzis and Shrimpton (2012)), in systems where transient charge injection is required (Kourmatzis and Shrimpton (2011)) and in heat transfer enhancement (Dantchi et al. (2013); Luo et al. (2016)). Numerous recent simulations have demonstrated the ability of EHD to advantageously modify heat transfer characteristics (Wu and Traore (2015); Dantchi et al. (2013); Wu et al. (2015)). In most of these problems the working fluid is an electrically insulating dielectric liquid, with an ionic mobility (κ) that is typically three orders of magnitude lower than air. This can make the ionic drift term κE_0 take on a magnitude that is of the same order of magnitude as the hydrodynamic component of the velocity U_0, where E_0 is the applied electric field. This condition suggests that there can be a two-way coupling in the flow, such that fluid flow can re-distribute space charge and hence influence the electric field. This is in contrast to the much simpler 'one-way' coupled EHD problems such as electrostatic precipitators which use air as a working fluid, and typically result in $\kappa E_0 >> U_0$ (Castellanos (1991)). EHD turbulence for one-way coupled problems has been examined by Soldati and Banerjee (1998) and experimental observations of such EHD turbulence are available (Atten. et al. (1997)).

In the case of two-way coupled EHD turbulence, one of the first systematic studies was by Hopfinger and Gosse (1971) who developed a simple eddy viscosity model and also demonstrated that the turbulent electrical energy is generally negligible in turbulent isotropic flows. Recent direct numerical simulations (DNS) by Kourmatzis and Shrimpton (2012) for hydrodynamically laminar, but electrohydrodynamically 'turbulent' flows confirmed this finding in the domain bulk, however demonstrated that E_i' plays a key role next to the injecting electrode, forming part of a main sink term in the turbulent scalar

flux transport equation. In the same contribution, free electroconvection was examined in three-dimensions for the first time, demonstrating that at an electric Reynolds number $Re_E \sim 60$ there is a broad distribution of length-scales in the flow which are markedly different from the standard electroconvective instabilities observed in two dimensions (Chicon et al. (1997); Vazquez et al. (2008)). This has significant implications in the design of charge injection devices. More recently, the energy cascade of AC induced electrokinetic (EK) turbulence was examined theoretically (Zhao and Wang (2017)). The authors theoretically demonstrated the effectiveness of EK in generating turublence and enhancing micro-mixing. Much of this work followed from experimental observations of electrokinetically induced turbulence in microfluidic flows (Wang et al. (2014)) showing the potential of EK turbulence to enhance the performance of these devices. For a more detailed review of turbulent electrohydrodynamics, and more specifically of the governing equations, the reader is directed to Kourmatzis and Shrimpton (2009) and Castellanos (1998).

While it is evident that some work has focused on describing the mechanisms that drive electrohydrodynamically induced turbulent mixing, the literature on the subject is sparse with a complete absence of knowledge on whether turbulence models can be used to close the problem of EHD turbulence. It was only recently that the full Reynolds averaged equations of EHD turbulence were made available in Kourmatzis and Shrimpton (2009) and Kourmatzis (2011). Through derivation of the averaged equations for turbulent EHD, it becomes apparent that there are a number of unclosed terms, where terms specific to the turbulent kinetic energy, scalar flux and variance budgets have been presented and discussed in Kourmatzis and Shrimpton (2012).

The aim of this paper is to test and develop closures for 'EHD-specific' terms containing electric field and charge fluctuations, particularly for non-linear terms which appear in the turbulent scalar flux, variance and Reynolds stress transport equations. Firstly, the Reynolds averaged forms of the relevant equations are presented and described and the simulation conditions briefly stated. Timescales relevant to the EHD problem which can be used within the closures tested are then briefly defined followed by a testing of

turbulence closures for the scalar flux and variance. Given zero imposed shear in this free convection problem (Kourmatzis and Shrimpton (2012)), contributions from the Reynolds stress are ignored. The paper concludes by examining the feasibility of closing higher order non-linear EHD terms.

2. Timescales and Governing Equations

A full description of the governing equations for electrohydrodynamics as applicable to pure incompressible dielectrics may be found in Kourmatzis and Shrimpton (2012, 2016) and Castellanos (1998) however they are reproduced here, for constant properties, with only brief statements describing their meaning. The governing equations for EHD flow can be written non-dimensionally with separate scales defining the bulk fluid velocity U_0 and the electric drift velocity κE_0, or in the case of free convection where $U_0 \sim \kappa E_0$ the equations reduce to a simpler form. Here, V is the voltage (volts), **with reference value V_0 such that $V^* = V/V_0$, U is the fluid velocity (m/s) where $U^* = U/U_0$, Q the space charge (C/kg) where Q^*/Q_0, t is the time (s) where $t^* = t/(l_0/U_0)$, and in these instantaneous governing equations, ϵ is the dielectric permittivity (F/m) with $\epsilon^* = \epsilon/\epsilon_0$.** If one ignores electrical diffusion as is common in electrohydrodynamic flows (due to the electrical Schmidt number $Sc_E >> 1$ as described in Kourmatzis and Shrimpton (2012)), then the space charge transport equation can be written without a diffusion term.

$$\frac{\partial}{\partial x_i^*}(U_i^*) = 0 \tag{1}$$

$$\frac{\partial}{\partial t^*}(U_i^*) + \frac{\partial}{\partial x_j^*}(U_i^* U_j^*) = \frac{1}{Re}\frac{\partial}{\partial x_j^*}\left(\frac{\partial U_i^*}{\partial x_j^*}\right) - \frac{\partial p^*}{\partial x_i^*} + \frac{Gr_E}{Re^2} Q^* E_i^* \tag{2}$$

$$\frac{\partial}{\partial t^*}(Q^*) + \frac{\partial}{\partial x_i^*}(U_i^* Q^*) = -\frac{\kappa_0 E_0}{U_0}\left(E_i^* \frac{\partial Q^*}{\partial x_i^*} + Q^{*2}\right) \tag{3}$$

$$\frac{\partial}{\partial x_i^*}\left(\epsilon^* \frac{\partial V^*}{\partial x_i^*}\right) = -Q^* C \tag{4}$$

where

$$Gr_E = \frac{\rho_0^2 Q_0 V_0 l_0^2}{\mu_0^2}, Re = \frac{\rho_0 U_0 l_0}{\mu_0}, \tag{5}$$

Equations 1 to 4 show the conservation of mass, momentum, space charge, and the Poisson equation for voltage respectively. Electrostrictive and dielectrophoretic forces are not considered as they are negligible for the simulation parameters used (Vazquez et al. (2008, 2006)).

In the free flow case U_0 may be referenced to κE_0 rather than U_0 and therefore the EHD momentum conservation equation has a different form (Kourmatzis and Shrimpton (2012)):

$$\frac{\partial}{\partial t^*}(U_i^*) + \frac{\partial}{\partial x_j^*}(U_i^* U_j^*) = -\frac{\partial p^*}{\partial x_i^*} + \frac{1}{Re_E}\frac{\partial^2 U_i^*}{\partial x_j^* \partial x_j^*} + CM^2 Q^* E_i^* \tag{6}$$

The C parameter is the injection strength term governing how 'strong' or 'weak' an injection is and is defined by equation 7 with $C >> 1$ being indicative of strong injection and $C << 1$ being indicative of weak injection. This term can also be defined as the ionic drift timescale τ_d to Coulombic charge relaxation timescale τ_{SC} ratio.

$$C = \frac{\rho_0 Q_0 l_0^2}{\epsilon V_0} = \frac{\tau_d}{\tau_{SC}} \tag{7}$$

where

$$\tau_d = \frac{l_0^2}{\kappa_0 V_0} \tag{8}$$

$$\tau_{SC} = \frac{\epsilon_0}{\rho_0 Q_0 \kappa_0} \tag{9}$$

and

$$M = \frac{(\epsilon/\rho_0)^{1/2}}{\kappa} = \left(\frac{T}{Re_E}\right)^{1/2}, Re_E = \frac{\rho\kappa V}{\mu} \tag{10}$$

The electrical Rayleigh number or the 'T' parameter is an indicator of electroconvective instability (Castellanos (1991, 1998)).

$$T = \frac{\epsilon V_0}{\kappa\mu} = Gr_E Pr_E \tag{11}$$

2.1. Timescales

Non-dimensionalization of the governing equations results in the appearance of a number of timescales (Kourmatzis and Shrimpton (2009)). The drift (τ_d) and relaxation (τ_{SC}) timescales were defined in section 2 and represent the time that it takes for a charge to decay from a given point in a dielectric, and the time that it takes for a fluid element to move a particular distance due to electroconvection, respectively. Of relevance to this contribution is to also note that if the electric field is scaled to the space charge through use of Gauss's law, as opposed to scaled to a voltage gradient, then the definition of τ_d becomes identical to τ_{SC}.

An additional timescale is the electro-inertial timescale $\tau_{ei} = l_0\sqrt{\frac{\rho}{\epsilon E_0^2}}$ being relevant where inertial forces are of the same order of magnitude as electrical forces. Of particular interest to note is that in the case of constant properties, τ_d and τ_{ei} will differ only through a constant defined by the ionic mobility, dielectric permittivity and density, given that τ_{ei} can be re-written as $\tau_{ei} = \frac{l_0^2}{V}\sqrt{\frac{\rho}{\epsilon}} = (\tau_d\kappa)\sqrt{\frac{\rho}{\epsilon}}$.

In the context of a turbulent flow, a turbulent timescale magnitude can be defined as the ratio of the turbulent kinetic energy to the rate of dissipation of the turbulent kinetic energy, and extending the definition to an electro-hydrodynamic flow, an analogous timescale may be defined as the turbulent electrical energy to the rate of dissipation of the turbulent electrical energy. The 'electrical dissipation' term in turbulent flows was only recently described in Kourmatzis and Shrimpton (2012) such that the turbulent electrical timescale is defined as in equation 12 where an overbar indicates an averaged term as described in Kourmatzis and Shrimpton (2012). **Briefly, the**

denominator of equation 12 **was identified as an electrical diffusion term in the transport equation of the turbulent electrical energy in Kourmatzis and Shrimpton (2012). While it was previously shown that the majority of turbulent electrical energy is converted to turbulent kinetic energy in the bulk, this diffusion term is used here as an analogous 'dissipation of the turbulent electrical energy' term, largely applicable close to walls where kinetic energy is low. The term is utilized here in order to make use of a timescale which is directly analogous to the ratio of turbulent kinetic energy to dissipation of turbulent kinetic energy.**

$$\tau_{tee} = \frac{\frac{1}{2}\epsilon\overline{E_2'^2}}{\mu\frac{\partial\overline{q'E_2'}}{\partial x_2}} = \frac{k_e}{\epsilon_e} \tag{12}$$

2.2. Averaged Transport Equations

The Reynolds averaged versions of the turbulent scalar variance and flux equations are shown in equations 13 and 14 and only include the significant terms as determined through the study of Kourmatzis and Shrimpton (2012). **Insignificant terms from the original turbulent scalar flux and variance equations were identified after a budget analysis from the DNS data as those terms that had a near-zero value or were orders of magnitude lower than the significant terms throughout the full length of the domain. The neglected terms make an insignificant contribution to the overall transport of turbulent scalar flux and variance in the case of free electroconvection (Kourmatzis and Shrimpton (2012)).** The final simplified equations are presented for the case of no mean flow and for the case where gradients are present only in one direction (direction '2'-also referred to herein as the 'vertical' direction). This simplification is employed here as we focus only on the situation of free convection between two parallel plates. Briefly, terms 1, 2 and 5 of equation 13 represent production of the scalar variance, and terms 3 and 6 are turbulent transport terms, with more complete descriptions provided in Kourmatzis and Shrimpton (2009). Term 6 is unclosed.

In the turbulent scalar flux equation (14), term 1 is a production term, term 2 a turbulent transport term (as it would appear in a scalar flux transport equation for a passive scalar), terms 3 and 5 are production and transport terms resulting from the ionic drift component, term 7 is a pressure-charge correlation (as it would appear for a passive scalar), and terms 8 and 9 are the diffusion of the scalar flux and a charge-field correlation term respectively. Terms 2 and 7 are unclosed.

$$\frac{\partial\overline{(q'^2/2)}}{\partial t}+\kappa\left[\underbrace{\frac{2\rho\overline{Q}\,\overline{q'^2}}{D_V}}_{1}+\underbrace{\overline{q'E_2'}\frac{\partial\overline{Q}}{\partial x_2}}_{2}+\underbrace{\overline{E_2}\frac{\partial(\overline{q'^2}/2)}{\partial x_2}}_{3}\right]+\underbrace{\overline{q'u_2'}\frac{\partial\overline{Q}}{\partial x_2}}_{5}+\underbrace{\frac{\partial}{\partial x_2}\overline{q'q'u_2'}}_{6}=0 \tag{13}$$

$$\frac{\partial\rho\overline{u_2'q'}}{\partial t}+\rho\underbrace{\overline{u_2'u_2'}\frac{\partial\overline{Q}}{\partial x_2}}_{1}+\underbrace{\frac{\partial\rho\overline{u_2'u_2'q'}}{\partial x_2}}_{2}+\rho\kappa\left[\underbrace{\overline{u_2'q'}\frac{\rho\overline{Q}}{D_V}}_{3}+\underbrace{\frac{\partial}{\partial x_2}(\rho\overline{E_2}\,\overline{q'u_2'})}_{5}\right]=-\underbrace{\overline{q'\frac{\partial p'}{\partial x_2}}}_{7}+(\mu+\frac{\mu}{Sc_Q})\left(\underbrace{\frac{\partial}{\partial x_2}\frac{\partial}{\partial x_2}\overline{q'u_2'}}_{8}\right)+\underbrace{\rho\overline{q'E_2'}\,\overline{Q}}_{9} \tag{14}$$

3. Application of Closures

Closures presented in this contribution are tested against the DNS data of case S2 presented in Kourmatzis and Shrimpton (2012). Briefly, this is a three-dimensional simulation of a dielectric liquid three-dimensional 'slab' between two parallel two-dimensional plates. **In particular, the simulation is one of free electro-convection which is analogous to thermal Rayleigh-Benard convection, and for that reason there is no mean flow here. No-slip conditions are used at both the top and bottom**

plates (walls) and all boundaries perpendicular to the plates form periodic boundary pairs in the 'x' and 'z' directions where 'y' is the vertical direction. Charge is injected at a row of control volumes located adjacent to the bottom wall boundary, and this method is used for reasons discussed in Kourmatzis and Shrimpton (2012, 2016). **The electric field is applied between the top and bottom parallel plates such that the top plate is at a zero reference voltage, with the bottom plate at the voltage necessary to achieve the dimensionless conditions described below. This is described in further detail in Kourmatzis and Shrimpton (2012)**. The electric Rayleigh number (T), Charge injection strength term (C) and electric Reynolds number (Re_E) of the simulation are $T = 500$, $C = 10$ and $Re_E = 60$ respectively. The spatial resolution of the mesh is equal to 0.54η where η is the Kolmogorov spatial microscale. The temporal resolution is equal to $0.1\tau_{kolm}$ where τ_{kolm} is the Kolmogorov timescale. This timescale was significantly smaller than the smallest electrical timescale in the flow (which was typically 3-4τ_{kolm}) and also ensured that Courant numbers did not exceed unity.

Before commencing the discussion on model closures the reader should note that many of the propositions made here, apply only under high Reynolds number and local isotropy conditions. While this is a common and correct assumption to make in many conventional flows, EHD flows that exhibit turbulent characteristics are found to be in a 'laminar' regime when considering the hydrodynamic Reynolds number (Vazquez et al. (2008, 2006); Chang et al. (2006)), and while this may suggest that these models are inappropriate close to walls, DNS has revealed a distribution of length-scales for electric Reynolds numbers $Re_E = 60$, which is equivalent to turbulent Rayleigh Benard convection (Kourmatzis and Shrimpton (2012)), and this suggests applicability of such models at lower equivalent hydrodynamic Reynolds numbers. The applicability of RSM models is demonstrated by this contribution.

3.1. Closure timescales

The reader should also note that the typical timescale used in Reynolds stress model closures is the ratio of turbulent kinetic energy (t.k.e.) to dissipation of t.k.e as shown

for instance in equation 15 as the ratio k/ϵ_k. We refer to this timescale as the 'Standard' timescale in this contribution however also test Reynolds stress closures using electro-hydrodynamic timescales given the well known coupling between turbulence generation and space charge (Castellanos (1998)). The timescales tested in the closures are the 'Standard timescale' (t.k.e./rate of dissipation of t.k.e), the drift timescale τ_d (equation 8), the space charge relaxation timescale τ_{SC} (equation 9) and the turbulent electrical timescale τ_{tee} (equation 12). The electro-inertial timescale τ_{ei} is not used in any closures given its scaling with the drift timescale, and this is evident through observation of Fig. 1.

Figure 1 demonstrates the variation of these timescales across the domain for statistically stationary conditions, where the averaging process has been explained in detail in Kourmatzis and Shrimpton (2012). In Fig. 1, τ_d and τ_{SC} have been calculated using the average values of q ($\overline{Q}$) and the average values of the voltage ($\overline{V}$) with the length-scale being the local mesh size in the vertical direction. Due to the non-linearity of charge across the domain it is clear that the electrodynamic timescales result in assymetric variation across the domain whereas the standard timescale is symmetric due to the symmetry in the turbulent kinetic energy (Kourmatzis and Shrimpton (2012)) but also near symmetry in the turbulent scalar flux of charge. The Standard, turbulent electrical energy timescale and space charge relaxation timescales are of a similar order of magnitude whereas the local drift timescale (defined using a potential gradient for the electric field) is seen to be several orders of magnitude lower near the bulk, however comparable to the other timescales near the injecting electrode. The timescale analysis suggests that model constants used to define an EHD closure should be of the same order of magnitude if defining the timescale either using the Standard, turbulent electrical energy, or space charge relaxation definitions.

3.2. Turbulent scalar variance models

In a scalar variance model the only term that requires closure is term 6 of equation 13, which is a conventional turbulent scalar variance transport term. This term may be modelled most simply using a Daly and Harlow approximation where the constant C_Q

is typically ~ 0.22, shown here with the Standard timescale (Daly and Harlow (1970)):

$$\overline{q'q'u_2'} \sim \frac{-C_Q k}{\epsilon_k}\left[\overline{u_2'^2}\frac{\partial \overline{q'q'}}{\partial x_2}\right] \tag{15}$$

Figure 2 plots the DNS value of $<< q'q'u_2' >>$ with the model closure of equation 15 with all timescales. The qualitative agreement with this particular third order moment is seen to be excellent however with the Standard timescale, use of a model constant significantly different from that quoted in the literature is required. This is not surprising, as there is high non-linearity in the space charge field, which appears to the second order in the scalar variance. Utilizing the model constant shown in the caption of figure 2 with a Standard timescale and traditional model (Daly and Harlow (1970)) yields an error range from a maximum of 70% close to the wall to an average error of 21% between y/L=0.2 and y/L=0.8, with errors less than 5% near the middle of the domain where the assumption of isotropy is reasonable. Qualitatively, the agreement is excellent and the profile of the closure captures the trends in the turbulent scalar variance even at $y/L < 0.2$ showing the model's suitability close to the walls. Constants for all of the timescales have been chosen here by optimizing the fit of the model through a reduction of the bulk average error (the bulk being defined from $0.2 < y/L < 0.8$). The error here is defined as the percentage difference in the local value of $\overline{q'q'u_2'}$ between DNS and model. The bulk average errors using τ_{tee}, τ_d, τ_{SC} as timescales in the model were calculated to be 30, 26 and 11% respectively, demonstrating superior performance of the model through use of a space charge relaxation timescale in this instance, which shows outstanding comparison to the DNS data above a $y/L = 0.5$ in comparison to the Standard timescale which is preferable below this value. **Close to the grounded electrode at y/L=1, the TEE and space charge relaxation timescale result in the best agreement to the DNS result, which is consistent with the consideration that electrical terms become more significant close to the wall, hence resulting in electrodynamic timescales being more relevant to the closure at that location**. Therefore, in this instance turbulence models for EHD can be optimized

through the use of a variable timescale, which for closure of this particular term, can reduce the overall average bulk average error in the domain to the order of $\sim 10\%$.

3.3. Turbulent scalar flux model closures

Terms that require closure from equation 14 are terms 2 and 7, which are conventional turbulent scalar flux transport terms and pressure scrambling terms respectively. Term 2 may be modeled using a Daly and Harlow model (Daly and Harlow (1970)) as follows:

$$\overline{u_2' u_2' q'} \sim \frac{-2C_S k}{\epsilon_k} \left[\overline{u_2'^2} \frac{\partial \overline{q' u_2'}}{\partial x_2} \right] \tag{16}$$

Equation 16 is in terms of the turbulent kinetic energy and dissipation. A typical model constant for this expression lies between $.05 < C_S < .11$ (Pope (2000)) for a Standard timescale, however Dol et al. (1997) have shown that this constant can take significantly higher values in RBC flows.

The pressure scrambling term (term 7 of equation 14) may be modelled as in Samaraweera (1978):

$$-\overline{\frac{q'}{\rho} \frac{\partial p'}{\partial x_i}} = -C_{QP} \frac{\epsilon_k}{k} \overline{q' u_i'} + C_{QP1} \overline{q' u_j'} \frac{\partial \overline{U_i}}{\partial x_j} \tag{17}$$

Where for the case of free convection between two plates this is re-written as:

$$-\overline{\frac{q'}{\rho} \frac{\partial p'}{\partial x_2}} = -C_{QP} \frac{\epsilon_k}{k} \overline{q' u_2'} \tag{18}$$

The value for the model constant C_{QP} is typically $C_{QP} \sim 3$ for thermal convection (Samaraweera (1978)).

The closure given by equation 16 is shown in figure 3. The agreement is qualitatively good though there is significant error. The model constants are chosen here so as to reduce the bulk average error. Dol et al. (1997) observed significant errors of the order 100% when using the Daly Harlow approximation with thermal convection, and this is reflected here in the case of electro-convection, with the closure result providing only a qualitative agreement with the DNS and being within the error bounds for RBC (Dol

et al. (1997); Chandra and Grotzbach (2008)). In Chandra and Grotzbach (2008), errors in higher order gradient terms of $\overline{\Phi' u_2' u_2'}$ could exceed 100% near to the walls and with significant errors also apparent in the domain bulk. For the EHD closure, the agreement up to y/L=0.1 is to within 5% for most timescale variants however increasing to errors which can locally exceed 100% between y/L=0.2 and y/L=0.5 which is comparable to the RBC literature. The average error between y/L=0.2 and y/L=0.8 is equal to 58 %, 63 %, 61 % and 67 % for the Standard, Drift, turbulent electrical and space charge relaxation timescales respectively, showing that the Standard timescale demonstrates slightly improved prediction which could be attributed to the turbulent transport term being more linked to changes in the local turbulent kinetic energy. The value of the model constant with use of a Standard timescale is equal to 0.04 with the literature quoting values between .05 and .11. **As with the space charge variance, the TEE and space charge relaxation timescales are to be preferred close to the grounded electrode.**

Figure 4 shows the scrambling closure of equation 18, and as with RSM closures for pressure scrambling in RBC flows (Dol et al. (1997); Chandra and Grotzbach (2008)) the error close to the wall can be significant, however what may be seen is that in the bulk where the isotropy assumption is valid, the agreement between the closures and the DNS values is excellent. In RBC scalar flux models, particularly in pressure scrambling models, it is common for the error between DNS and model closure to reach its minimum after approximately y/L=0.2 (Dol et al. (1997); Chandra and Grotzbach (2008)) and this is observed here for EHD as well using most of the timescale definitions. Between y/L=0.2 and 0.8 the error is an average of 7.4% for a Standard timescale which is an excellent agreement for an RSM model, and results in the best comparisons with DNS data showing that in the near isotropic region of the flow the turbulent kinetic energy to dissipation ratio is the most pertinent flow timescale. The other timescales result in errors ranging from 10% (drift) to 47% (with τ_{tee}). The model constant for the Standard timescale $C_{QP} = 6.5$ is within the same order of magnitude as the $C_{QP} = 3.0$ quoted in the literature (Samaraweera (1978)) showing that pressure scrambling may

be modeled using conventional RSM closures with widely accepted constants. The fact that the closures are in good agreement in the centre of the domain also further suggests that EHD case S2 has features that do resemble a turbulent flow, given that an isotropy assumption in the domain bulk results in good model estimates. The straight application of an RSM model for pressure scrambling without any significant change to the model constant compared to what is used for conventional flows suggests a certain degree of universality between Rayleigh-Benard and free electrohydrodynamic convection in the transport of turbulent scalar flux transport by the pressure term.

4. The EHD triple correlation

In EHD there is strong non-linearity in the space charge field, which, coupled to the electric field, affects the velocity distribution through a Lorentz force on the conservation of momentum equation. This coupling of momentum, charge and electric field also appears explicitly in the averaged equations as a third order moment term $\overline{q'u_2'E_2'}$. This term appears as a triple correlation in the full turbulent scalar flux equation and similar triple correlations appear in the transport equation for shear stress, not shown here, however the contribution of these triple correlations to the overall flux and shear is minimal (Kourmatzis and Shrimpton (2012)). Nevertheless, it is of fundamental interest to determine if a triple correlation containing both fluctuating field and velocity components coupled to scalar fluctuations can be modeled, as this will have implications in other types of turbulent EHD flows. In most conventional turbulent scalar flux models the only relevant vector is that of velocity, however given that in charge injection systems there is a scalar flux contribution both from ionic drift and bulk convection velocities, the problem is significantly more complicated.

The authors follow the modeling strategy of Daly and Harlow (1970), and based on energy, scalar flux and variance contributions shown in Kourmatzis and Shrimpton (2012), it is apparent that terms containing the turbulent scalar flux $\overline{q'u_2'}$ are generally more significant than $\kappa\overline{q'E_2'}$ in the bulk of the domain. Therefore, the initial assumption made is that the transport of the triple correlation term is mainly attributed to gradients

in the turbulent scalar flux $\overline{q'u_2'}$ where a correlation $\overline{u_2'E_2'}$ is used as a diffusion coefficient through the following closure, termed 'closure 1':

$$\overline{q'u_2'E_2'} = -C_U \frac{k}{\epsilon_k} \overline{u_2'E_2'} \frac{\partial \overline{q'u_2'}}{\partial x_2} \tag{19}$$

An alternative closure, termed 'closure 2' would be to assume that both the gradients in the turbulent scalar flux $\overline{q'u_2'}$ and $\kappa\overline{q'E_2'}$ contribute in which case the model is changed to:

$$\overline{q'u_2'E_2'} = -C_{U1} \frac{k}{\epsilon_k} \left[\underbrace{\overline{u_2'E_2'} \frac{\partial \overline{q'u_2'}}{\partial x_2}}_{A1} + \underbrace{\kappa \overline{u_2'E_2'} \frac{\partial \overline{q'E_2'}}{\partial x_2}}_{A2} \right] \tag{20}$$

The results of the closures of equations 19 and 20 show nearly identical results due to the minimal contribution of term 'A2' from closure 2 and therefore only 'Closure 1' is shown here in figure $5(a)$ alongside the DNS data for the various timescale definitions. Model constants chosen for Fig. $5(a)$ are shown in the caption with bulk average errors ranging from 25 to 51%. More specifically, the standard, turbulent electrical and space charge relaxation timescales yield comparable errors of the order of 25-30%. Closure 1 is incapable of recovering the DNS data accurately from the region of $y/L = 0.2$ to $y/L = 0.4$. The location of y/L=0.2 physically corresponds to where the gradient of mean space charge vs. y/L experiences a significant decrease, and incidentally this is also the physical location where for a typical Rayleigh-Benard flow, the bulk temperature gradient approaches zero. RBC models have also been shown to deviate from DNS data in this region.

In addition to equations 19 and 20 already suggested for this triple correlation, an additional closure is presented. An assumption made is that in addition to $\overline{u_2'E_2'}$ acting as a 'diffusion coefficient' a contribution is also present from $\overline{u_2'^2}$ which is a significant term, and it is assumed that this acts on the ionic drift turbulent scalar flux contribution ($\kappa\overline{q'E_2'}$). **The added contribution of $\overline{u_2'^2}$ is merited given that it is known from DNS simulations Kourmatzis and Shrimpton (2012) that this is the most sig-**

nificant contributor to the Reynolds stress tensor, and the key contributing component to the turbulent kinetic energy, which drives much of the flow physics throughout the solution domain. Utilizing this term as a diffusion coefficient to $\frac{\partial \overline{q'E_2'}}{\partial x_2}$ is therefore a direct way to examine the influence of coupling between the turbulent kinetic energy and the scalar flux of charge driven by the ionic drift velocity. This closure ('closure 3') is shown in equation 21 and results in an interesting finding.

$$\overline{q'u_2'E_2'} = -C_{U3}\frac{k}{\epsilon_k}\left[\overline{u_2'E_2'}\frac{\partial \overline{q'u_2'}}{\partial x_2} + \overline{u_2'u_2'}\frac{\partial \overline{q'E_2'}}{\partial x_2}\right] \tag{21}$$

Figure 5(b) shows the results from equation 21, and although a qualitative agreement is seen, the error is in excess of 200% throughout the bulk. However, a significant feature of the model is that it can capture the y-intercept at $y/L \sim 0.18$, such that below y/L=0.18, closure 3 is in excellent agreement, while above a y/L=0.42, closure 2 is a better approximation, and this is generally true regardless of the timescale used in the model definition. This indicates that closer to the bottom wall, a term resembling the gradient of the turbulent scalar flux by the electric field ($\overline{q'E_2'}$) is proportional to the third order transport term through a component of the turbulent kinetic energy $\overline{u_2'u_2'}$, the latter being defined as a turbulent normal stress 'diffusion coefficient'. Whilst this is only a model closure, it indicates the statistical coupling that occurs between the turbulent kinetic energy and turbulent flux terms. **As with the space charge variance and flux closures, once again the TEE and space charge relaxation timescales result in a reduced error close to the grounded electrode, showing consistently that across a variety of transport terms electrodynamic timescales are particularly relevant in regions of low turbulent kinetic energy.**

These results suggest that the model closures of equations 19 and 21 may be combined in order to give a better overall representation of the transport of this triple correlation. This is demonstrated in Fig. 6 using a Standard timescale, given reasonable results with this timescale from closures 1 and 3. In region A of Fig. 6, closure 3 is used, in region B the average of closure 1 and 3 is used, and in region C closure 1 is used. An

average is used in zone B as it is apparent from observing Fig. 5(a) that this would yield reasonable estimates. This approach yields a very good qualitative agreement and in the cases nearer to the walls results in excellent quantitative agreements with errors below 5%. The model confirms that higher order non-linear EHD terms can be modelled using Reynolds stress closures by making use of varying turbulent diffusion coefficients throughout the domain, and this includes near the wall. These models implicitly account for varying contributions from electrical and hydrodynamic terms.

5. Conclusions

Reynolds stress closure strategies for the modeling of turbulent EHD flow have been analyzed and tested for the first time. Multiple timescale definitions have been used in the model definitions with a Standard timescale (t.k.e/rate of dissipation of t.k.e) resulting in the most consistent quantitative accuracy however the space charge relaxation, drift and turbulent electrical energy based timescales have also provided reasonable estimates. Turbulent scalar flux, turbulent scalar variance, Reynolds stress and a triple correlation term specific to EHD were closed with model formulations which have been used in the past for thermal convection. The turbulent scalar variance and turbulent scalar flux closures were the most accurate with an average error of approximately 21% for the scalar variance and an average error in the bulk of approximately 7.4% for the pressure scrambling closure with Standard timescales. These error magnitudes are comparable to closures available for RBC flow. The results show a degree of consistency with RBC models in that turbulent fluxes at certain locations (e.g. adjacent to the initial charge layer at $\sim$y/L=0.2) are difficult to accurately predict with an RSM approach. Reynolds stress closures applied to the triple correlation specific to EHD confirmed that complex third order moment profiles may be modeled; though the strategy is more complex, and requires a dynamic change in the turbulent diffusion coefficient when moving away from the bottom (injecting) wall of the domain. This contribution represents the first work available in the literature to suggest and test modeling strategies for turbulent electrohydrodynamic flows. Future work is recommended in the modeling of chaotic and

turbulent EHD flows that have a bulk convective flow.

References

J. Shrimpton, A. Yule, Atomization, combustion, and control of charged hydrocarbon sprays, Atomization and Sprays 11 (2001) 1–32.

J. S. Shrimpton, A. J. Yule, Characterization of charged hydrocarbon sprays for application in combustion systems, Experiments in Fluids 26 (1999) 460–469.

J. S. Shrimpton, A. J. Yule, Design issues concerning charge injection atomizers, Atomization and Sprays 14 (2004) 127–142.

A. Kourmatzis, J. Shrimpton, Electrohydrodynamic inter-electrode flow and liquid jet characteristics in charge injection atomizers, Experiments in Fluids 55 (2014).

A. Kourmatzis, E. L. Ergene, J. S. Shrimpton, D. C. Kyritsis, F. Mashayek, M. Huo, Combined aerodynamic and electrostatic atomization of dielectric liquid jets, Experiments in Fluids 53 (2012) 221–235.

D. C. Kyritsis, B. Coriton, F. Faure, S. Roychoudhury, A. Gomez, Optimization of a catalytic combustor using electrosprayed liquid hydrocarbons for mesoscale power generation, Combustion and Flame 139 (2004) 77 – 89.

A. Kourmatzis, J. Shrimpton, Primary atomization and drop size characteristic of an electrostatic dielectric liquid pulsed atomizer, Atomization and Sprays 22 (2012) 351–370.

A. Kourmatzis, J. Shrimpton, Electrical and transient atomization characteristics of a pulsed charge injection atomizer using electrically insulating liquids, Journal of Electrostatics 69 (2011) 157 – 167.

K. Dantchi, T. Philippe, R. Hubert, W. Jian, L. Christophe, Numerical simulations of electro-thermo-convection and heat transfer in 2d cavity, Journal of Electrostatics 71 (2013) 341 – 344.

K. Luo, J. Wu, H.-L. Yi, H.-P. Tan, Lattice boltzmann modelling of electro-thermo-convection in a planar layer of dielectric liquid subjected to unipolar injection and thermal gradient, International Journal of Heat and Mass Transfer 103 (2016) 832 – 846.

J. Wu, P. Traore, A finite-volume method for electro-thermoconvective phenomena in a plane layer of dielectric liquid, Numerical Heat Transfer, Part A: Applications 68 (2015) 471–500.

J. Wu, P. Traore, A. T. Perez, P. A. Vazquez, On two-dimensional finite amplitude electro-convection in a dielectric liquid induced by a strong unipolar injection, Journal of Electrostatics 74 (2015) 85 – 95.

A. Castellanos, Coulomb-driven convection in electrohydrodynamics, IEEE Trans. Elect. Insulation 26 (1991) 1201–1215.

A. Soldati, S. Banerjee, Turbulence modification by large-scale organized electrohydrodynamic flows, Physics of Fluids 10 (1998) 1742–1756.

P. Atten., B. Malraison, M. Zahn, Electrohydrodynamic plumes in point-plane geometry, IEEE Trans. Dielectrics Elect. Insulation 4 (1997) 710718.

E. J. Hopfinger, J. P. Gosse, Charge transport by self-generated turbulence in insulating liquids submitted to unipolar injection, Physics of Fluids 14 (1971) 1671–1682.

A. Kourmatzis, J. S. Shrimpton, Turbulent three-dimensional dielectric electrohydrodynamic convection between two plates, Journal of Fluid Mechanics 696 (2012) 228–262.

R. Chicon, A. Castellanos, E. Martin, Numerical modelling of coulomb-driven convection in insulating liquids, Journal of Fluid Mechanics 344 (1997) 46–66.

P. Vazquez, G. Gheorgiou, A. Castellanos, Numerical analysis of the stability of the electrohydrodynamic (EHD) electroconvection between two plates, Journal of Physics D: Applied Physics 41 (2008).

W. Zhao, G. Wang, Scaling of velocity and scalar structure functions in ac electrokinetic turbulence, Phys. Rev. E 95 (2017) 023111.

G. Wang, F. Yang, W. Zhao, There can be turbulence in microfluidics at low reynolds number, Lab on a Chip 14 (2014) 1452–1458.

A. Kourmatzis, J. Shrimpton, Electrohydrodynamics and charge injection atomizers: a review of the governing equations and turbulence, Atomization and Sprays 19 (2009) 1045–1063.

A. Castellanos, Basic Concepts and Equations in Electrohydrodynamics in : Electrohydrodynamics 1st ed. (editor: Castellanos, A), Springer-Verlag, 1998.

A. Kourmatzis, Pulsed Charge Injection Atomization and Turbulent Electrohydrodynamics, Ph.D. thesis, University of Southampton, 2011.

A. Kourmatzis, J. S. Shrimpton, Characteristics of electrohydrodynamic roll structures in laminar planar couette flow, Journal of Physics D: Applied Physics 49 (2016) 045503.

P. A. Vazquez, G. E. Gheorgiou, A. Castellanos., Characterization of injection instabilities in electrohydrodynamics by numerical modelling: comparison of particle in cell and flux corrected transport methods for electroconvection between two plates, J.Phys. D 39 (2006).

J. Chang, D. Brocilo, K. Urashima, J. Dekowski, J. Podlinski, J. Mizeraczyk, G. Touchard, On-set of EHD turbulence for cylinder in cross flow under corona discharges, Journal of Electrostatics 64 (2006) 569–573.

B. Daly, F. Harlow, Transport equations in turbulence, Physics of Fluids 13 (1970) 2634–2649.

S. Pope, Turbulent Flows, Cambridge University Press, 2000.

H. Dol, K. Hanjalic, S. Kenjeres, A comparative assessment of the second-moment differential and algebraic models in turbulent natural convection, International Journal of Heat and Fluid Flow 18 (1997) 4–14.

D. Samaraweera, Turbulent heat transport in two and three dimensional temperature fields, Ph.D. thesis, Imperial College London, 1978.

L. Chandra, G. Grotzbach, Analysis and modelling of the turbulent diffusion of turbulent heat fluxes in natural convection, International Journal of Heat and Fluid Flow 29 (2008).

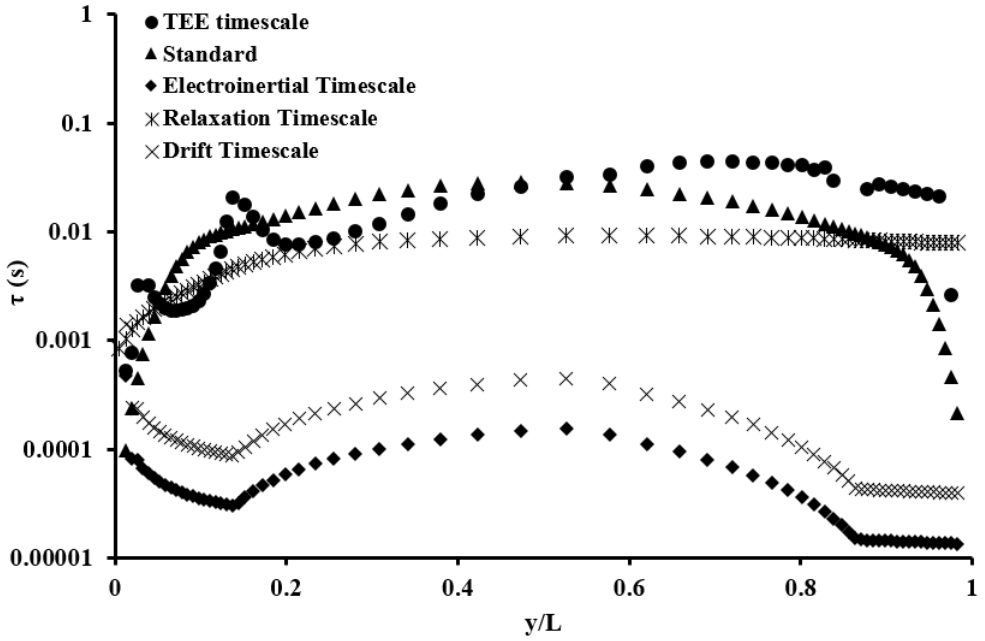

Figure 1: Local timescale magnitudes plotted vs dimensionless vertical location across solution domain

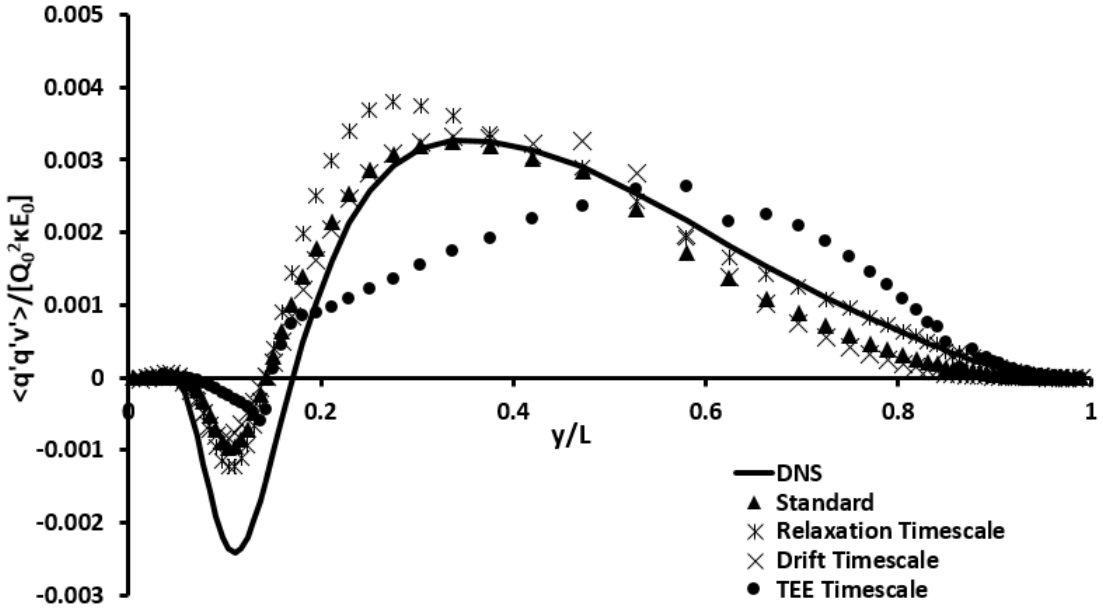

Figure 2: Turbulent scalar variance transport from DNS case S2 plotted with model closure of equation 15 *with* $C_Q = 0.05$ *for Standard timescale,* $C_Q = 0.05$ *for* τ_{tee} *timescale,* $C_Q = 0.16$ *for* τ_{SC} *timescale and* $C_Q = 3.8$ *for the drift timescale.*

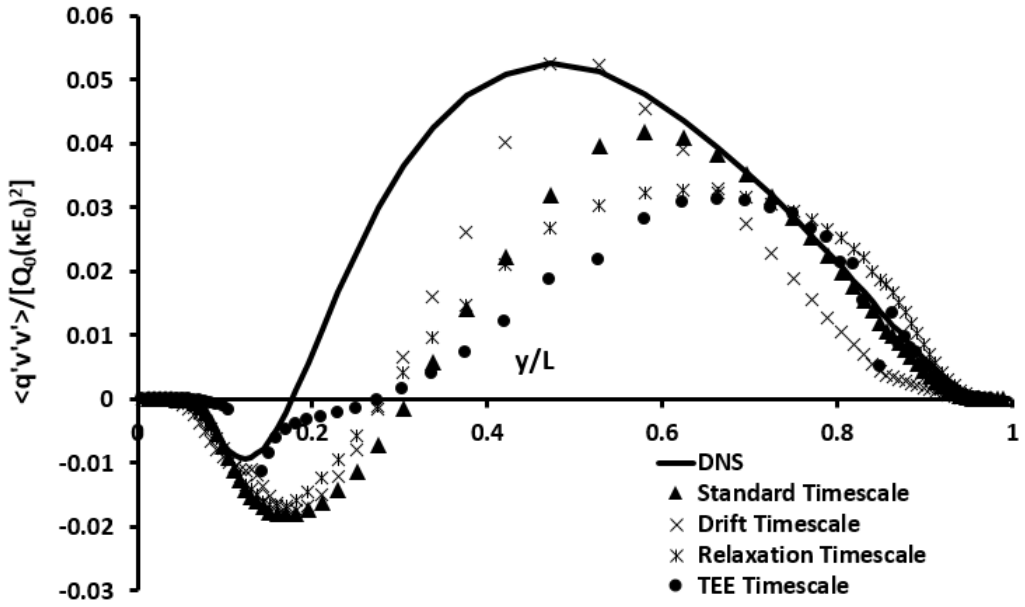

Figure 3: Turbulent scalar flux transport term ($<< q' u_2' u_2' >>$) of equation 14 *from DNS case S2 plotted with model closure of equation* 16 *vs.* y/L *with* $C_S = 0.07$ *for Standard timescale,* $C_S = 0.03$ *for* τ_{tee} *timescale,* $C_S = 0.15$ *for* τ_{SC} *timescale and* $C_S = 6$ *for the drift timescale*

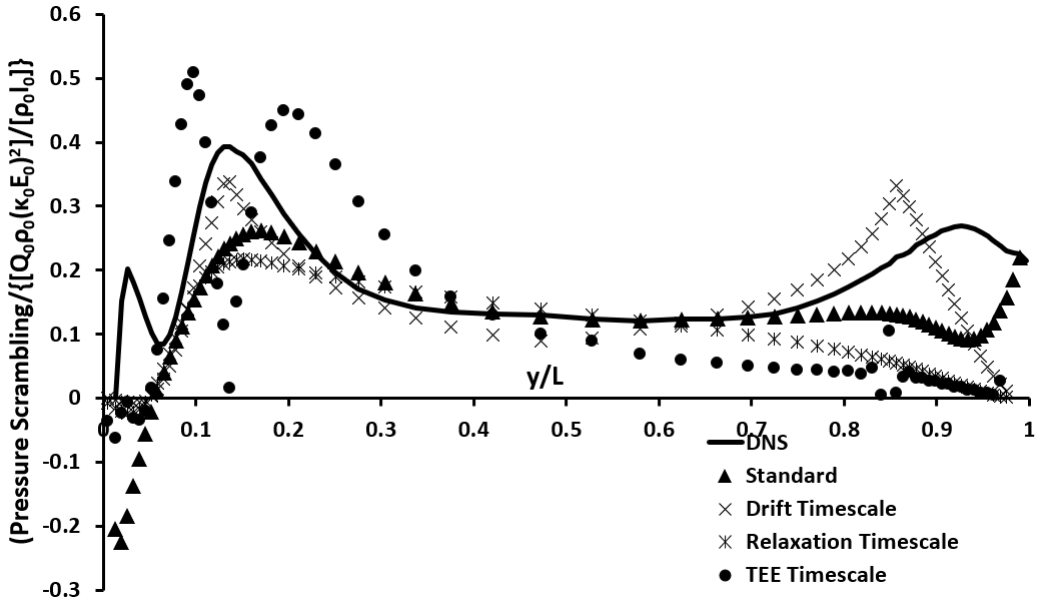

Figure 4: Pressure scrambling term of equation 14 *from DNS case S2 alongside model closure of equation* 18 *vs.* y/L *with* $C_{QP} = 6.5$ *for Standard timescale,* $C_{QP} = 6$ *for* τ_{tee} *timescale,* $C_{QP} = 2.4$ *for* τ_{SC} *timescale and* $C_{QP} = .075$ *for the drift timescale*

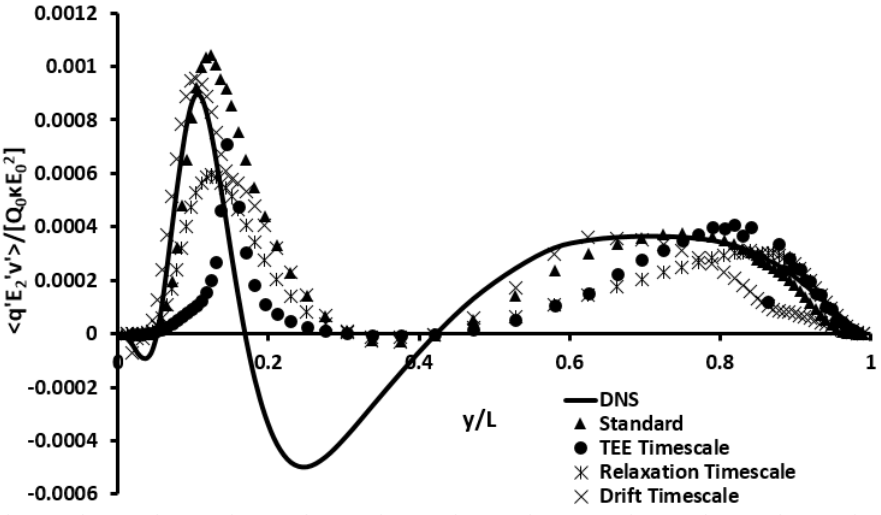

(a) $<< q'E_2'u_2' >>$ vs. y/L with $C_U = 0.024$ for Standard timescale, $C_U = 0.01$ for τ_{tee} timescale, $C_U = 0.035$ for τ_{SC} timescale and $C_U = 2$ for the drift timescale

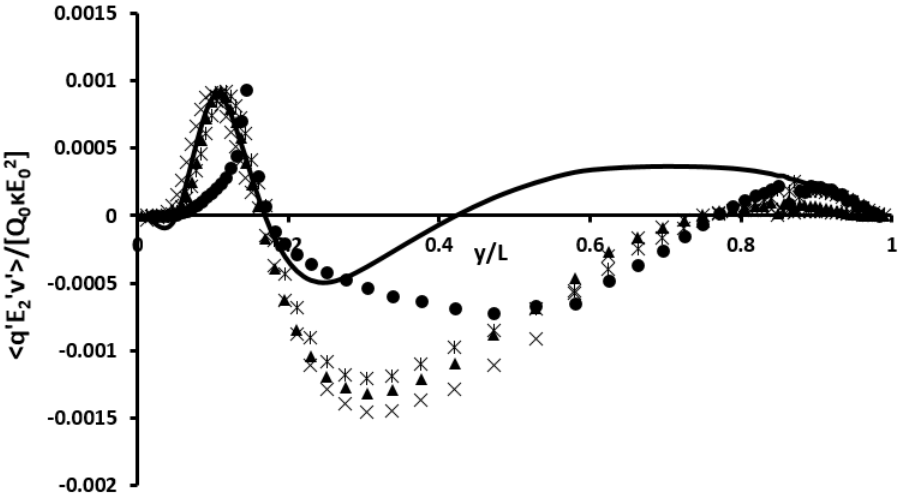

(b) $<< q'E_2'u_2' >>$ vs. y/L with $C_{U3} = 0.03$ for Standard timescale, $C_U = 0.025$ for τ_{tee} timescale, $C_U = 0.074$ for τ_{SC} timescale and $C_U = 2.5$ for the drift timescale

Figure 5: Triple correlation $\overline{q'E_2'u_2'}$ from DNS case S2 plotted with model closures of equations 19 (a) and 21 (b)

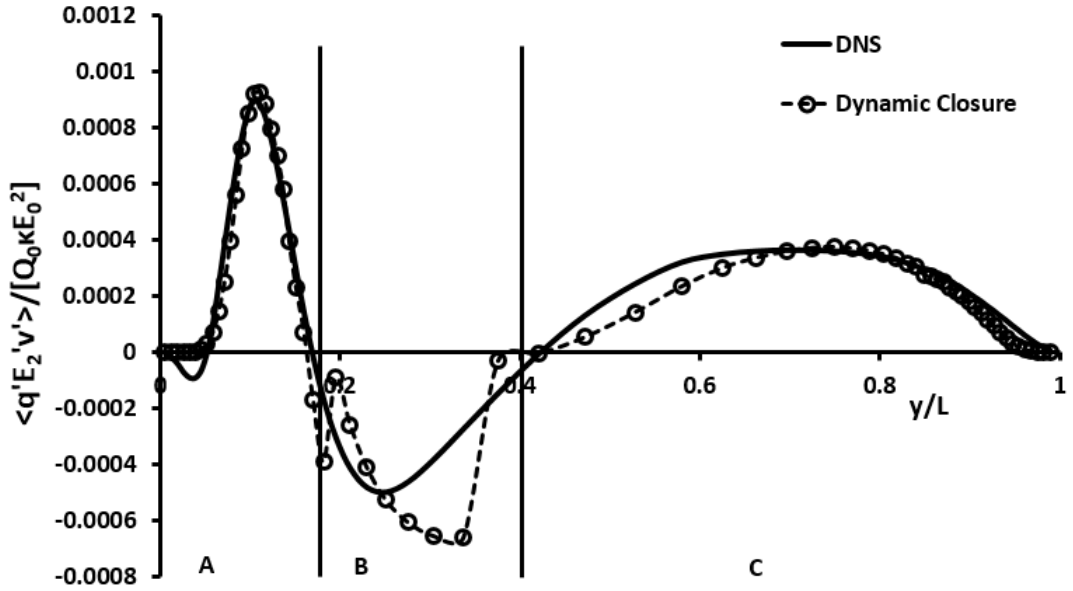

Figure 6: $<< q' E_2' u_2' >>$ vs. y/L with a dynamic closure and Standard timescale with a model constant of 0.03